

# Quantum state tomography of an itinerant squeezed microwave field

F. Mallet,<sup>1</sup> M. A. Castellanos-Beltran,<sup>1,2</sup> H. S. Ku,<sup>1,2</sup> S. Glancy,<sup>3</sup> E. Knill,<sup>3</sup> K. D. Irwin,<sup>3</sup> G. C. Hilton,<sup>3</sup> L. R. Vale,<sup>3</sup> and K. W. Lehnert<sup>1,2,\*</sup>

<sup>1</sup>*JILA, National Institute of Standards and Technology and the University of Colorado, Boulder, CO 80309, USA*

<sup>2</sup>*Department of Physics, University of Colorado, Boulder, CO 80309, USA*

<sup>3</sup>*National Institute of Standards and Technology, Boulder, Colorado 80305, USA*

(Dated: October 28, 2018)

We tomographically reconstruct the Wigner function of an itinerant squeezed state of the microwave field prepared by a Josephson parametric amplifier (JPA). We use a second JPA as a pre-amplifier to improve the quantum efficiency of the field quadrature measurement (QM) at microwaves from 2 % to  $36 \pm 4$  %. Without correcting for the detection inefficiency we observe a minimum quadrature variance which is  $68_{-7}^{+9}$  % of the variance of the vacuum, where the uncertainty is mostly caused by systematic uncertainty in calibrating the QM. Using a maximum likelihood method to account for detection inefficiency, we infer the variance of the squeezed quadrature to be  $48_{-19}^{+45}$  % of the vacuum's variance.

PACS numbers: 42.50.Dv, 42.50.Lc, 03.67.Bg

Keywords: Josephson parametric amplifier, squeezed state, quantum state tomography

Fundamental quantum optics experiments at microwave frequencies have been recently performed with superconducting qubits or Rydberg atoms inside high-quality microwave cavities. Examples include the reconstruction of the Wigner functions of Fock states from one [1] to a few photons and coherent superpositions of few photons [2–4]. States such as these, which are manifestly nonclassical light states, are crucial for quantum information processing, because they can be used to generate entanglement. However, in the cited experiments, these states are confined in cavities. Therefore distributing entanglement to separate parties, as required in quantum communication protocols, remains challenging for microwave implementations. In contrast to the discrete Fock state approach, continuous variables quantum information (CVQI) strategy uses another type of nonclassical states, the squeezed states, which are readily created in itinerant modes. These states exhibit reduced noise, below the vacuum fluctuations, in one of their quadrature components and amplified noise in the other one. They are also easily generated at optical frequencies in the itinerant output modes of parametric amplifiers made of optically nonlinear crystals. At optical frequencies, CVQI has progressed rapidly from the initial creation of squeezed states [5] and tomographic reconstruction [6–8] of those states to teleportation [9, 10] and quantum error correction [11, 12].

At microwave frequencies, the field is less advanced. The generation of microwave squeezed states using the nonlinear electrical response of superconducting Josephson junctions has been reported [13], with inferred squeezing down to 10 % of vacuum variance [14]. Such states can be powerful tools for quantum information processing and communication because microwaves and superconducting qubits can mimic useful light–atom interactions, as demonstrated in [15]. Furthermore, these

devices are made of compact and integrable electrical circuits, with much promise for building complex quantum information processors. The lack of an efficient quadrature measurement (QM) for itinerant modes has slowed the advancement of CVQI. However, as demonstrated recently in [16], it is possible with a JPA to realize an efficient single QM.

In this Letter, we report the tomography of an itinerant squeezed microwave field. We demonstrate that our JPA based measurement scheme has a quantum efficiency 20 times greater than a QM employing state-of-art semiconductor amplifiers. We infer the quantum state prepared by maximum likelihood tomography, correcting for inefficiency in our QM. We discuss the achieved degree of squeezing, from the perspective of generating entanglement on chip.

Homodyne tomography is a standard experimental tool to infer the quantum state of a single mode of light. It was as proposed in [17] and pioneered on a squeezed optical field in [6]. Its principle is depicted in the Fig. 1. A homodyne detection apparatus measures the value of the quadrature  $X_\theta$ , where  $\theta$  is set by adjusting the phase of the local oscillator. The probability density functions  $\text{pr}(X_\theta)$  for measuring a particular value of  $X_\theta$  is the projection of the Wigner function on to the vertical plane defined in the quadrature phase space by the polar angle  $\theta$ , as shown in Fig. 1 (b). Thus by performing measurements of  $X_\theta$  on many identical copies of the system and varying  $\theta$ , the “hidden” quantum object can be seen from different angles and its state inferred. Losses and other Gaussian noise sources in the homodyne detector can be modeled with the insertion of a fictitious beam splitter of transmissivity  $\eta$ , as shown in Fig. 1 (a). In such a case, the measured  $\text{pr}(X_\theta)$  are no longer the projections of the desired Wigner function but of a smoother quasiprobability distribution created by convolution of the de-

sired Wigner function with a Gaussian Wigner function [18]. However methods like maximum likelihood quantum state tomography can be used to deconvolve the effect of inefficiency.

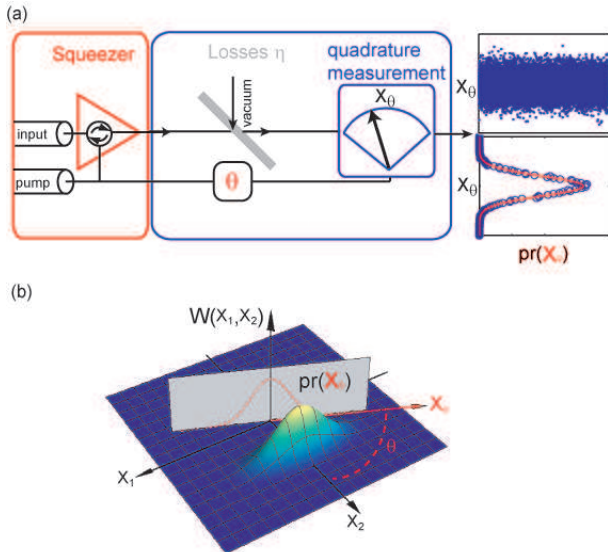


FIG. 1: Principle of the experiment. (a-left): The squeezer (SQ, in red) prepares a squeezed state whose quadrature distributions are measured for different phases  $\theta$  with an efficiency  $\eta$ . (a-right): Simulated measurement results for 20,000 realizations of creating the squeezed state and measuring it at a single  $\theta$ . The top graph shows the measured quadrature value versus realization number. The bottom plot is a histogram (blue circles) and Gaussian probability distribution  $\text{pr}(X_\theta)$  (red curve) of this random process. (b): Graphical Interpretation: the probability distribution  $\text{pr}(X_\theta)$  is simply the projection of the Wigner function:  $\text{pr}(X_\theta) = \int dX_{\theta+\pi/2} W(X_\theta, X_{\theta+\pi/2})$ .

At optical frequencies,  $\eta \geq 90\%$  is routinely obtained using a pair of balanced photodiodes [19]. Such detectors are not available for microwaves and until recently the best setup was a chain of phase-insensitive amplifiers followed by a mixer, or two such chains in parallel [20, 21]. In such a case, noise  $A_n$  greater than  $1/2$  (the vacuum variance) must be added to the quadrature measurements [22]. This noise can be modeled as an effective efficiency by the relation  $\eta = 1/(1 + 2A_n)$  [23], so the QM efficiency using phase-insensitive amplifiers is limited to 50%. State of the art microwave amplifiers, high-electron-mobility transistors (HEMTs), have  $A_n \approx 10 - 20$ . Including the unavoidable losses present in a microwave experiment, in practice  $\eta$  is of the order of 0.02. However, as demonstrated in [16], inserting a JPA used as a single quadrature preamplifier before the HEMT increases the experimentally achieved  $\eta$  by a factor of approximately 20.

To perform a high-quality reconstruction of the Wigner function of a squeezed microwave state we operate two JPAs, as shown in Fig. 2 (b). The first JPA, referred to

as the squeezer (SQ), prepares the squeezed state. The second JPA, referred to as the pre-amplifier (AMP), amplifies the quadrature of the squeezed state determined by the phase difference  $\theta$  between the AMP and the SQ pump tones. We vary  $\theta$  by applying to the two cavities pump tones slightly detuned from one another. The SQ stage is pumped at 7.45 GHz, while the AMP stage is pumped at 100 kHz higher frequency; therefore, sweeping  $\theta$  through  $2\pi$  every 10  $\mu\text{s}$ .

Our implementation of an SQ or an AMP at microwaves, as shown in Fig. 2 (a), requires three elements: (i) a JPA used in reflection, (ii) a directional coupler and (iii) a circulator. As described in [14], the JPAs are either quarter-wave or half-wave resonant cavities built from coplanar waveguides whose central conductor has been replaced by a series of many Josephson junctions. The Josephson junctions' nonlinearity causes the cavity's phase velocity to be intensity dependent. Therefore when the cavity is pumped it becomes a phase sensitive amplifier for input modes whose frequencies lie within the bandwidth of the JPA centered on the pump frequency. Such microwave modes incident on the JPA are reflected and exit the cavity with one quadrature amplified and the other squeezed, depending on their phase relative to the pump's phase. A directional coupler allows the pump to enter through the weakly coupled port while the reflected signal simply flows through the direct port. The reflected signal consists of amplified and squeezed modes displaced from the origin of phase space by the reflected pump tone. That displacement is approximately removed by applying the appropriate tone to the isolated port of the directional coupler, so that the reflected pump tone is canceled by interference. Finally the incident and reflected modes are separated into different cables using a circulator.

Following Fig. 2 (b), in the limit of large HEMT power gain  $G_H$ , our quantum efficiency can be cast as

$$\eta = \frac{\alpha}{1 + 2(A_A + (1 - \alpha)/2 + (A_H + (1 - \beta)/2)/G_A\beta)}, \quad (1)$$

where  $A_A$  ( $A_H$ ) is the AMP (HEMT) added noise,  $\alpha$  ( $\beta$ ) is the fraction of power transmitted by the microwave circuitry between the SQ and the AMP (the AMP and the HEMT), and  $G_A$  is the power gain of the AMP stage. A detailed description of how we calibrate each of these parameters is in the supplementary information. The general strategy is to put thermal noise at different temperatures into the different segments of the circuit in Fig. 2, operate each JPA either as an amplifier (ON) or as a noiseless element with unit gain (OFF), and observe the variation in the noise at the output of the measurement chain. A microwave switch connects the input of the SQ to either a "hot load" (50  $\Omega$  microwave termination at 4.1 K) or a "cold load" (at 20 mK), preparing the modes in the cable in the corresponding thermal state. Although the tomography of the squeezed state is only

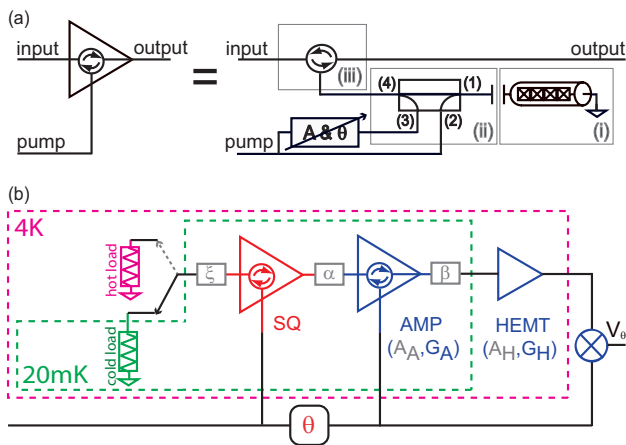


FIG. 2: (a): To implement a SQ or AMP at microwaves, three microwave components are required: (i) a JPA, (ii) a directional coupler and (iii) a circulator. Taking the port (1) of the directional coupler as reference, (2) is the weakly coupled port, (3) the isolated port and (4) the direct port. (2) is used to pump the JPA, and on port (3), the displacement of the output of the JPA, back to the origin of the phase space, is performed with a pair of room temperature attenuator and phase shifter. (b): Schematics of the experiment. In this figure, switch, circulators, directional couplers and the cables connecting all the different microwave devices are considered lossless; their imperfection have been taken into account in the experimentally determined total transmissivities  $\xi$ ,  $\alpha$  and  $\beta$ .

performed with the “cold load”, both are required for calibration. We obtain  $A_A = 0.25 \pm 0.06$ ,  $A_H = 17.3 \pm 0.1$ ,  $\alpha = -1.7 \pm 0.1$  dB and  $\beta = -1.3 \pm 0.3$  dB. However, as the (lossy) switch is operated at the 4.1 K stage, the state presented at the input of the SQ with the “cold load” is not pure quantum vacuum, but a low occupancy thermal state with average photon number  $\bar{n} \simeq 0.15 \pm 0.15$ . One quadrature of the squeezed state is then amplified at the AMP stage with sufficient gain  $G_A = 180$  such that the noise in the amplified quadrature exceeds  $A_H$  for any  $\theta$ . According Eq. (1), we obtained an overall quantum efficiency of  $36 \pm 4$  %, which can be compared to  $\eta \approx 2$  % without the AMP stage.

In this experiment our uncertainty in  $\eta$  and  $\bar{n}$  create a systematic source of error. We thus perform our data analysis under three assumptions (1) high efficiency ( $\eta = 0.40$ ) and high mean photon number ( $\bar{n} = 0.30$ ), (2) best estimate for both efficiency ( $\eta = 0.36$ ) and mean photon number ( $\bar{n} = 0.15$ ), and (3) low efficiency ( $\eta = 0.33$ ) and low mean photon number ( $\bar{n} = 0$ ). These three cases give us “pessimistic”, “best-guess”, and “optimistic” analyses. Associated with each of these three cases, we also have statistical uncertainty, so the given error bounds cover an interval that includes both uncertainties around the “best-guess” estimate.

We must also calibrate the effective gain of the QM. In optical homodyne tomography, this is usually done

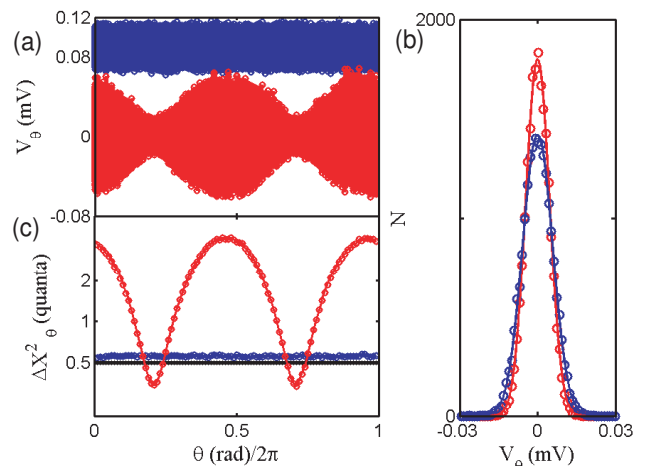


FIG. 3: (a): Measured voltage  $V_\theta$  of the amplified quadrature of the AMP versus the reduced phase difference  $\theta/2\pi$  with the SQ pump OFF (top, shifted up 0.09 mV for clarity, blue) and ON (red). (b): Histograms of  $V_\theta$  at the maximum of squeezing: data (o) and Gaussian fit (continuous lines) for the SQ pump OFF (blue) and ON (red). (c): Noise variance  $\Delta X_\theta^2$  in quanta units on a log scale versus  $\theta/2\pi$  for the SQ pump ON (red) and OFF (blue). The (black) dashed line indicates our estimate of the vacuum noise level under the “best-guess” calibration.

by inserting the vacuum and observing the quadrature noise. Analogously, we insert the weak thermal state with mean photons  $\bar{n}$  (by simply turning the SQ pump OFF) and measure voltages proportional to quadrature values at many  $\theta$ , as shown (in blue) in Fig. 3. As expected this voltage noise is  $\theta$  independent, with a variance  $\Delta V_{SQ,OFF}^2 = 3.2 \times 10^{-5}$  mV<sup>2</sup>. Under the convention that vacuum has variance 1/2 in unitless quadrature space (or in units of “quanta”), we calibrate this voltage variance to  $\Delta X_{SQ,OFF}^2 = (1 - \eta)/2 + \eta(1/2 + \bar{n}) = 0.55^{+0.07}_{-0.05}$  quanta. Therefore the effective gain  $G_{sys} = \Delta X_{SQ,OFF}^2 / \Delta V_{SQ,OFF}^2 = 1.71^{+0.20}_{-0.17} \times 10^4$  quanta/mV<sup>-2</sup> is used to rescale the variances in Fig. 3 (c).

Experimental data of the squeezed state is shown in red in Fig. 3 (a). When the SQ pump in ON (red) we observe the characteristic phase dependent noise for a squeezed state. At the phase for which the variance is minimum, we show the histogram of quadrature measurements in Fig. 3 (b). The SQ OFF histogram is clearly wider than the SQ ON histogram, demonstrating our ability to observe squeezing directly at the output of our measurement chain. In Fig. 3 (c) we plot the variance of the QM with SQ ON and OFF as a function of  $\theta$ , expressed in units of quanta, clearly showing squeezing below the vacuum level. Without correcting for  $\eta$ , we observe a minimum quadrature variance which is  $68^{+9}_{-7}$  % of the variance of the vacuum.

To infer the quantum state created by the squeezer, correcting for loss during the QM, we used maximum like-

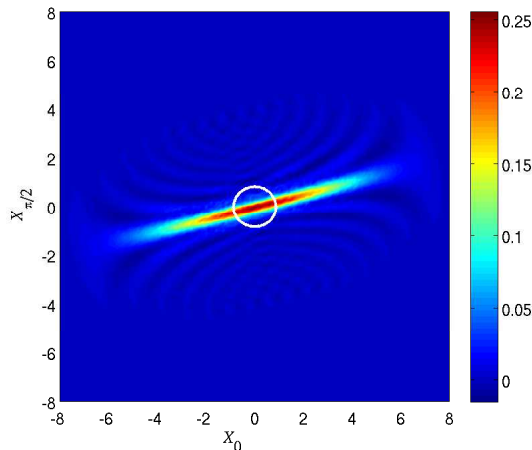


FIG. 4: Wigner function of state produced by the SQ, inferred by maximum likelihood with our “best-guess” calibration parameters. To represent statistical uncertainty in this figure, each pixel value is randomly chosen from a normal distribution whose mean is the mean of the pixel values found in 35 independent reconstructions, and whose variance is the variance of the 35 pixel values. The faint pattern of ripples extending from the origin is caused by truncation of the density matrix at 30 photons used to represent the state. The white circle at the origin shows the full-width at half-maximum of the vacuum state.

likelihood quantum state tomography [24]. For each of the three calibration cases, we performed 35 reconstructions using independent subsets each containing 10,000 QMs of the total measured data. We estimated statistical uncertainty from the spread of properties (such as fidelity or minimum variance) of the set of 35 reconstructions. The statistical uncertainty was significantly lower than the systematic uncertainty (See the supplementary information for more detail). Our estimates of the squeezed state’s properties are reported in the form  $X_{-L}^{+U}$ , where  $X$  is the mean of the 35 maximum likelihood estimates based on the “best-guess” calibration parameters.  $L$  and  $U$  are the lower and upper bounds of the one standard deviation uncertainty interval associated with our maximum likelihood estimate based on the “pessimistic” and “optimistic” cases.

In Fig. 4 we show the Wigner function of the “best-guess” reconstructed state. The pure squeezed state that has highest fidelity with our state has minimum quadrature variance  $6.0_{-1.1}^{+1.4}$  % of the vacuum variance, and the maximum fidelity achieved is  $0.81_{-0.17}^{+0.16}$ . However, the experimental state’s squeezed quadrature is actually  $48_{-19}^{+45}$  % of the vacuum’s variance, and the anti-squeezed quadrature’s variance is  $20.2_{-1.0}^{+5.4}$  times the vacuum variance. For comparison, the most highly squeezed optical state ever made has a variance of only 7 % of the vacuum variance [25].

Producing squeezed states of itinerant microwave

modes allows the generation of distributable entanglement by sending two copies of a squeezed vacuum state through the two input ports of a balanced beam splitter. The coherent information [26] is one useful way to characterize the entanglement between the two output modes. The asymptotic number of maximally entangled qubit pairs (e-bits) that can be distilled per copy of the noisy entangled state, by using local operations and one-way classical communication, is at least as large as the coherent information [27]. Given two copies of the squeezed state produced in our system, one could make two entangled modes with  $2.5_{-0.4}^{+1.0}$  e-bits of coherent information.

In conclusion, we have reconstructed the Wigner function of an itinerant squeezed microwave field generated at the output of a Josephson Parametric Amplifier. Using a second JPA as a preamplifier has increased the quantum efficiency of the microwave homodyne detection from approximately 2 % to 36 %. The level of squeezing is primarily limited by noise added to the squeezed state by the JPA. Improving the performance of the JPAs (as both squeezers and phase-sensitive amplifiers) will require more detailed investigation of the source of this noise. We used maximum likelihood quantum state tomography to deconvolve the QM inefficiency in order to precisely characterize the state generated. This is an important step towards generating easily distributable microwave entanglement on chip.

The authors acknowledge support from the DARPA/MTO QuEST program.

---

\* Electronic address: konrad.lehnert@jila.colorado.edu

- [1] A. A. Houck et al., *Nature* **449**, 328 (2007).
- [2] S. Deléglise et al., *Nature* **455**, 510 (2008).
- [3] M. Hofheinz et al., *Nature* **454**, 310 (2008).
- [4] M. Hofheinz et al., *Nature* **459**, 546 (2009).
- [5] R. E. Slusher et al., *Phys. Rev. Lett.* **55**, 2409 (1985).
- [6] D. T. Smithey et al., *Phys. Rev. Lett.* **70**, 1244 (1993).
- [7] S. Schiller et al., *Phys. Rev. Lett.* **77**, 2933 (1996).
- [8] G. Breitenbach, S. Schiller, and J. Mlynek, *Nature* **387**, 471 (1997).
- [9] A. Furusawa et al., *Science* **282**, 706 (1998).
- [10] H. Yonezawa, S. L. Braunstein, and A. Furusawa, *Phys. Rev. Lett.* **99**, 110503 (2007).
- [11] T. Aoki et al., *Nature Physics* **5**, 541 (2009).
- [12] M. Lassen et al., *Nature Photonics* **4**, 700 (2010).
- [13] B. Yurke et al., *Phys. Rev. Lett.* **60**, 764 (1988).
- [14] M. A. Castellanos-Beltran et al., *Nature Physics* **4**, 929 (2008).
- [15] A. Wallraff et al., *Nature* **431**, 162 (2004).
- [16] J. D. Teufel et al., *Nature Nanotechnology* **4**, 820 (2009).
- [17] K. Vogel and H. Risken, *Phys. Rev. A* **40**, 2847 (1989).
- [18] U. Leonhardt and H. Paul, *Phys. Rev. A* **48**, 4598 (1993).
- [19] A. I. Lvovsky and M. G. Raymer, *Rev. Mod. Phys.* **81**, 299 (2009).
- [20] D. Bozyigit et al. (2010), arXiv:1002.3738v1.
- [21] E. P. Menzel et al., *Phys. Rev. Lett.* **105**, 100401 (2010).

- [22] C. M. Caves, Phys. Rev. D **26**, 1817 (1982).
- [23] U. Leonhardt and H. Paul, Phys. Rev. Lett. **72**, 4086 (1994).
- [24] Z. Hradil et al., in Quantum State Estimation (2004), pp. 59–112.
- [25] M. Mehmet et al., Phys. Rev. A **81**, 013814 (2010).
- [26] B. Schumacher and M. A. Nielsen, Phys. Rev. A **54**, 2629 (1996).
- [27] I. Devetak and A. Winter, Proc. R. Soc. A **462**, 207 (2005).